European Spine Journal (2020) 29:670–685
https://doi.org/10.1007/s00586-019-06223-7

ORIGINAL ARTICLE

ISSLS PRIZE IN BASIC SCIENCE 2020: Beyond microstructure—circumferential specialization within the lumbar intervertebral disc annulus extends to collagen nanostructure, with counterintuitive relationships to macroscale material properties

Tyler W. Herod[1] · **Samuel P. Veres**[1,2]

Received: 11 October 2019 / Revised: 11 October 2019 / Accepted: 15 November 2019 / Published online: 25 November 2019

Abstract

Purpose To determine whether the annulus of lumbar intervertebral discs contains circumferential specialization in collagen nanostructure and assess whether this coincides with functional differences in macroscale material properties.

Methods Anterior and posterior disc wall samples were prepared from 38 mature ovine lumbar segments. Regional differences in molecular thermal stability and intermolecular network integrity of the annulus' tension-bearing collagen fibres were examined with hydrothermal isometric tension (HIT) analysis, with and without preceding $NaBH_4$ treatment to stabilize labile crosslinks. Energetics of collagen denaturation were studied by differential scanning calorimetry (DSC). Tensile mechanics of annular lamellae were studied using oblique sagittal bone-disc-bone samples loaded to rupture. Annular failure characteristics of the ruptured test segments were compared via microscopy of serial sections.

Results HIT showed that tension-bearing collagen fibres of the posterior annulus were composed of collagen molecules with significantly greater thermal stability and intermolecular network integrity than those of the anterior annulus. $NaBH_4$ treatment confirmed that labile intermolecular crosslinks did not significantly contribute to network integrity in either region. Regional differences seen in DSC were smaller than those observed in HIT, indicating structural similarities in annular collagen outside of the main fibre bundles. Mechanical testing showed that the posterior annulus was significantly *weaker* than the anterior annulus. For both regions, ultimate tensile strengths of annular fibres were significantly greater than those previously reported. Ruptures in both regions were predominantly due to annular failure.

Conclusion Specializations in collagen nanostructure exist between different circumferential regions of the annulus and coincide with significant differences in material properties.

Graphic abstract

These slides can be retrieved under Electronic Supplementary Material.

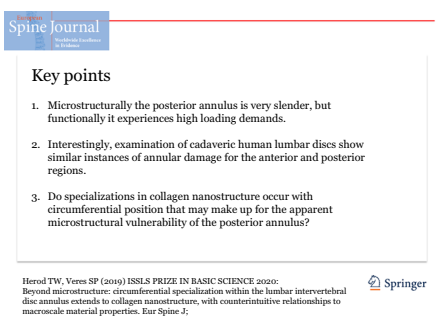

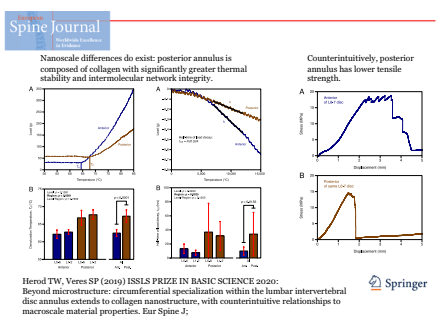

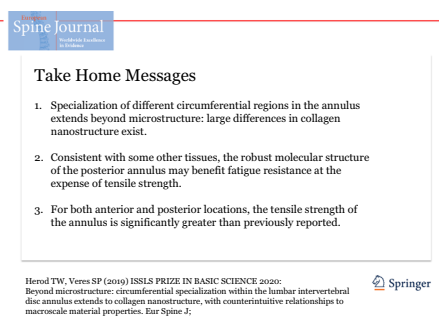

Electronic supplementary material The online version of this article (https://doi.org/10.1007/s00586-019-06223-7) contains supplementary material, which is available to authorized users.

Extended author information available on the last page of the article

Keywords Intervertebral disc annulus · Collagen nanostructure · Mechanical properties · Microscopy · Failure morphology · Structure–function

Introduction

From a microstructural standpoint, the posterior region of the lumbar disc wall seems ill-equipped to undertake its functional duty when compared to other circumferential regions. In terms of function, the posterior region is clearly charged with the most important job of all circumferential regions: to protect the spinal cord and nerve roots from mechanical compression or chemical irritation by migrating nuclear material. This requirement is made difficult by the common postures adopted during daily living. Bending at the waist flexes the spine, forcing the nucleus back against the posterior annulus [1, 2]. Despite knowing we ought not to, frequently enough one finds themselves applying force via the arms in this posture, perhaps lifting a child from the floor or pulling a tire iron, further pressurizing the nucleus [3]. Adding a slight twist places the posterior disc wall in additional jeopardy [4, 5], further straining those annular fibres oriented in the twist's direction and simultaneously increasing their responsibility for restraining the nucleus as counter-oriented annular fibres are relaxed. Given the level of disability that can result from failure, one would think that the posterior annulus would have evolved a robust structure to accommodate these frequently encountered loading scenarios.

Compared to other circumferential regions, the posterior annulus cannot be described as possessing a particularly robust microstructure. In relation to the anterior annulus, the posterior annulus contains significantly fewer lamellae [6] and is significantly thinner in total radial depth [7]. With the most slender portion of the disc wall experiencing significant functional loading [8], it is somewhat surprising that the incidence of structural damage to the disc's posterior is not greater. For instance, Moore et al. [9] examined parasagittal sections of 383 lumbar discs and found no difference in the incidence of rim lesions or radial tears between the anterior and posterior annulus. Osti et al. [10] similarly examined 135 discs and, while noting more radial tears in the posterior than anterior annulus, also noted that circumferential tears were seen equally in both regions and that rim lesions occurred more frequently in the anterior. Vernon-Roberts et al. [11] mapped structural alterations at L4–5 using parasagittal sections from 70 discs and noted only modestly higher incidences of radial tears, circumferential tears, and rim lesions in the posterior versus anterior disc wall at all ages.

Specialization of collagenous tissues to particular mechanical loading regimes often extends beyond the microscale, to smaller structural levels within the collagen hierarchy. For example, within the four valves of the heart, the molecular packing density of collagen varies according to the in vivo transvalvular pressure supported [12]. Anatomically proximate tendons that support differing in vivo loads show several significant differences in collagen nanostructure, including differences in collagen fibril diameter, molecular packing, and intermolecular crosslinking [13, 14]. Such nanostructural differences are accompanied by functional differences in collagen fibril mechanics and structural disruption resistance [15–17], which at the macroscale appear to directly influence properties such as fatigue resistance [13, 18].

For the intervertebral disc annulus, there are limited data available on whether collagen nanostructure varies with circumferential region and hence how differences in annular microstructure may be buttressed at finer levels of the collagen hierarchy in order to help meet functional demands. The current study was designed to determine whether the disc annulus does show any circumferential specialization in collagen nanostructure, and provide a better assessment of whether any such specializations are accompanied by functional differences in macroscale material properties. We find that significant differences in collagen nanostructure exist between the anterior and posterior annulus and that these differences coincide with large differences in resistance to tensile rupture.

Materials and methods

All numerical data are given as mean ± standard deviation.

Lumbar spines of mature ewes at least two years old were collected from a local abattoir within 24 h of slaughter. Spines were dissected into vertebra-disc-vertebra segments, wrapped in phosphate-buffered saline (PBS)-soaked gauze, and stored in freezer bags at − 86 °C to await the sample preparations described below.

Hydrothermal isometric tension (HIT) analysis

HIT analysis was used to explore whether differences in collagen molecule stability and intermolecular network integrity exist between anterior and posterior regions of the disc wall.

Native samples

The L1–2 and L5–6 discs of ten spines were used ($n = 10$). Spinal segments were retrieved from storage at − 86 °C and

thawed to room temperature. Residual soft tissues attached to the disc were carefully removed by scalpel, including the posterior longitudinal ligament. Using a miniature hacksaw, oblique sagittal bone-disc-bone samples were removed from the anterior and posterior regions of each segment, with cuts oriented parallel to the angle of annular fibres at the disc periphery (Fig. 1). The angle of the oblique cuts, measured using a digital bevel, was 32° ± 5° from the transverse plane for anterior samples, and 39° ± 5° from the transverse plane for posterior samples, consistent with previously reported values for the annular fibre inclination [19]. The average circumferential width and radial depth of the prepared samples were 3.22 ± 0.54 mm and 5.21 ± 1.15 mm, respectively.

HIT analysis was performed using a custom-built apparatus similar to that described previously by Lee et al. [20]. Briefly, each bone-disc-bone sample was longitudinally suspended between a load cell and fixed support using small clamps attached to the bone at either end. Mounted samples were then submerged in a bath of room-temperature distilled, deionized water. A tensile preload of 60 g was applied to each sample, after which samples remained isometrically constrained for the remainder of the test. Using a hot plate, the water bath was gradually heated to 90 °C and maintained under computer-controlled isotherm at this temperature for five hours while time, temperature, and load data were recorded at 0.2 Hz.

HIT data were analysed to determine each sample's denaturation temperature, T_d, and half-time of load decay, $t_{1/2}$. Denaturation temperature, a measure of collagen molecular stability, was marked in the temperature ramp data by the start of pronounced tensile load generation with increasing temperature (Fig. 2). Half-time of load decay, a measure of intermolecular network integrity, was calculated using the isothermal data by fitting a 5000-s data interval with a Maxwell decay (Fig. 3), as previously described [12].

Of the 40 samples prepared, four samples slipped during testing leaving 36 measurements of denaturation temperature. An additional four anterior samples were too large, requiring that the tests be terminated prior to the isothermal segment in order to avoid overloading the load cells.

$NaBH_4$-treated samples

To assess whether divalent, thermally labile crosslinks contributed to intermolecular network integrity in either region, HIT tests were also run using anterior and posterior samples that had been treated with the crosslink reducing agent sodium borohydride ($NaBH_4$).

The L1–2 and L2–3 discs from five spines were used ($n = 5$). Samples were prepared as described above for the native samples (Fig. 1). The average circumferential width and radial depth of the samples were 3.50 ± 0.56 mm and 4.40 ± 0.49 mm, respectively. From each spine, samples from the L1–2 disc were treated with $NaBH_4$ following the procedure previously described by Wells et al. [21]. Samples from the L2–3 discs served as animal-paired, untreated controls. $NaBH_4$ treatment consisted of four 15-min washes in 100 mL borate buffer solution containing 0.1 mg/mL $NaBH_4$ (pH = 9.0) under constant agitation at 4 °C, followed by three 10-min agitated rinses in distilled, deionized water at 4 °C. Matching samples from L2–3 discs underwent the same process, but without $NaBH_4$ added to the borate buffer. To ensure efficacy of the $NaBH_4$ treatment, samples of bovine forelimb digital extensor tendon, known to contain predominantly thermally labile crosslinks [13], were also prepared (Supplementary Figure S1). All samples then underwent HIT analysis as described above.

Differential scanning calorimetry (DSC)

DSC was used to explore further variations in collagen molecular stability within the annulus, with radial depth examined in addition to circumferential location.

The L4–5 or L5–6 discs from ten spines were used ($n = 10$). Anterior and posterior bone-disc-bone samples were prepared as described for the HIT samples (Fig. 1). Posterior samples measured 4.8 ± 0.5 mm in the circumferential direction and 5.2 ± 0.6 mm in the radial direction. The same measurements for the anterior samples were 4.9 ± 0.7 mm and 6.9 ± 0.7 mm. After overnight storage at 4 °C in distilled, deionized water, samples were further dissected in preparation for DSC. The annulus of each sample was first isolated from the superior and inferior endplates using a razor blade. Posterior samples were divided in half by a coronal cut, producing inner posterior and outer posterior samples. To account for their larger radial depth, anterior samples were similarly cut but in thirds, the middle third of which was discarded leaving inner anterior and outer anterior samples. From each of the four sampling locations, small subsamples were cut, weighed (average mass 10.42 ± 1.30 mg), and gently pressed into the bottom of aluminium DSC sample pans. Pans were hermetically sealed and run against an empty pan using a Q200 differential scanning calorimeter (TA Instruments, New Castle, DE) from 30 to 90 °C at 5 °C/min. On completion, sample pans were pierced and dried under vacuum. Weight measurements were taken every 24 h until stable in order to calculate each sample's dry mass.

DSC data were analysed using Universal Analysis 2000 software (version 4.5A, TA Instruments), with the following parameters extracted for each endotherm (Fig. 4): onset temperature (T_{onset}), peak temperature (T_{peak}), full width at half maximum ($FWHM$), and specific enthalpy of denaturation calculated using dry sample mass (Δh). Results from replicate subsamples were averaged prior to statistical analysis.

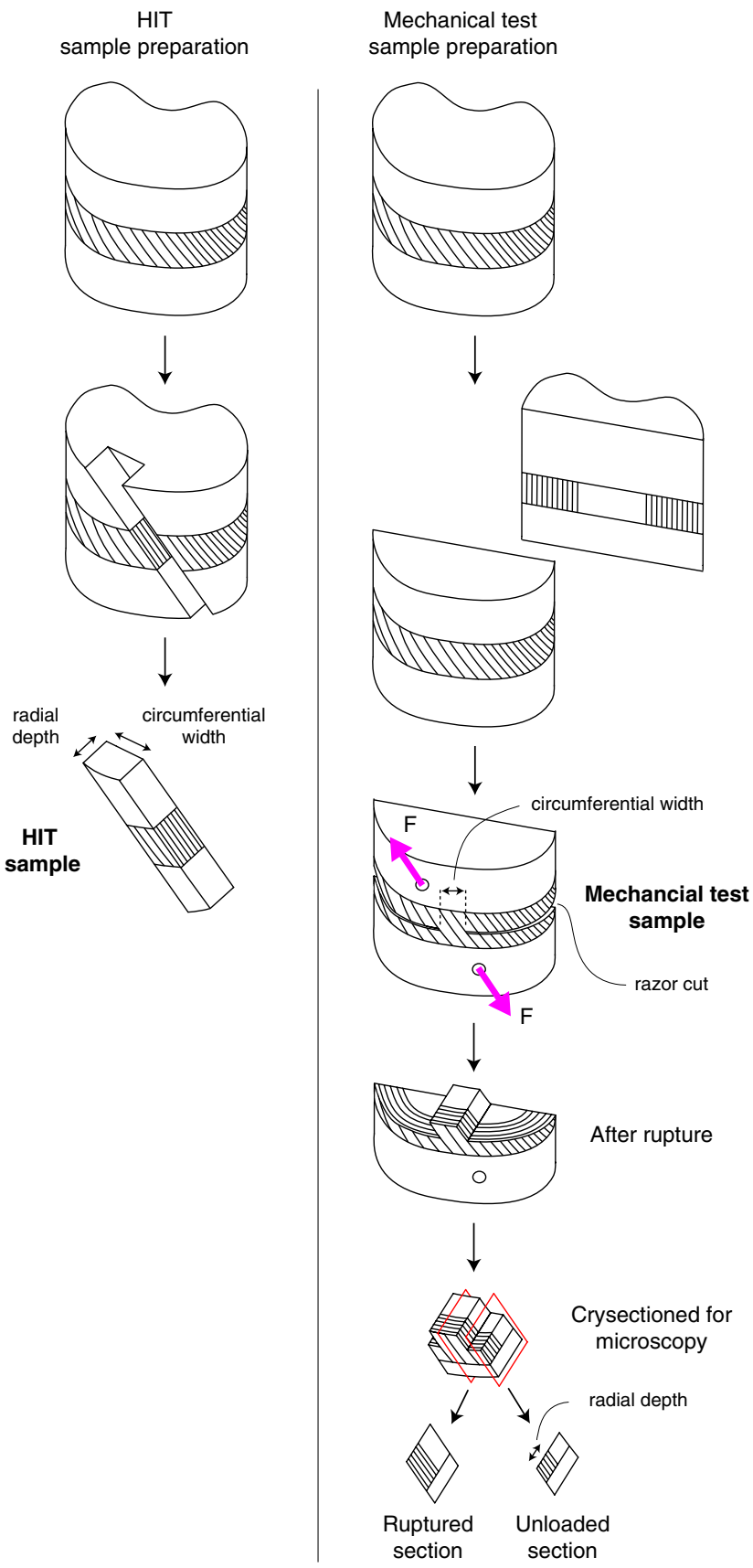

Fig. 1 Preparation of samples for hydrothermal isometric tension (HIT) analysis and mechanical testing. For HIT and mechanical testing, both the anterior and posterior portions of each disc were prepared and tested, with subsequent statistical analyses performed using these disc-matched pairings. For DSC, sample preparation proceeded as shown for HIT but with additional cuts made to isolate the annulus from the attached pieces of vertebrae, and then to subdivide the isolated annulus by radial depth

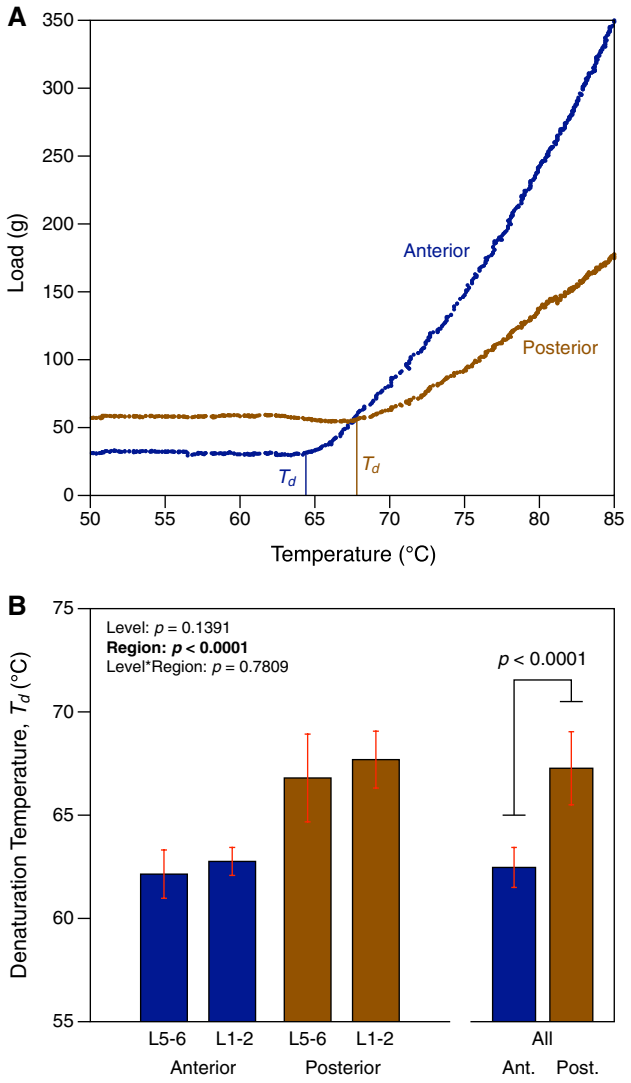

Fig. 2 Thermal stability of collagen molecules making up the posterior annulus was significantly greater than for those making up the anterior annulus, regardless of lumbar disc level. **a** Representative HIT responses showing thermal stability measurements via denaturation temperature (T_d) for anterior and posterior samples from the same L1–2 disc. **b** Results of the two-way mixed model ANOVA are shown inset. With neither the factor of level nor the interaction term significant, data after pooling of levels is shown on the right with corresponding significance for disc-matched-pair *t*-test

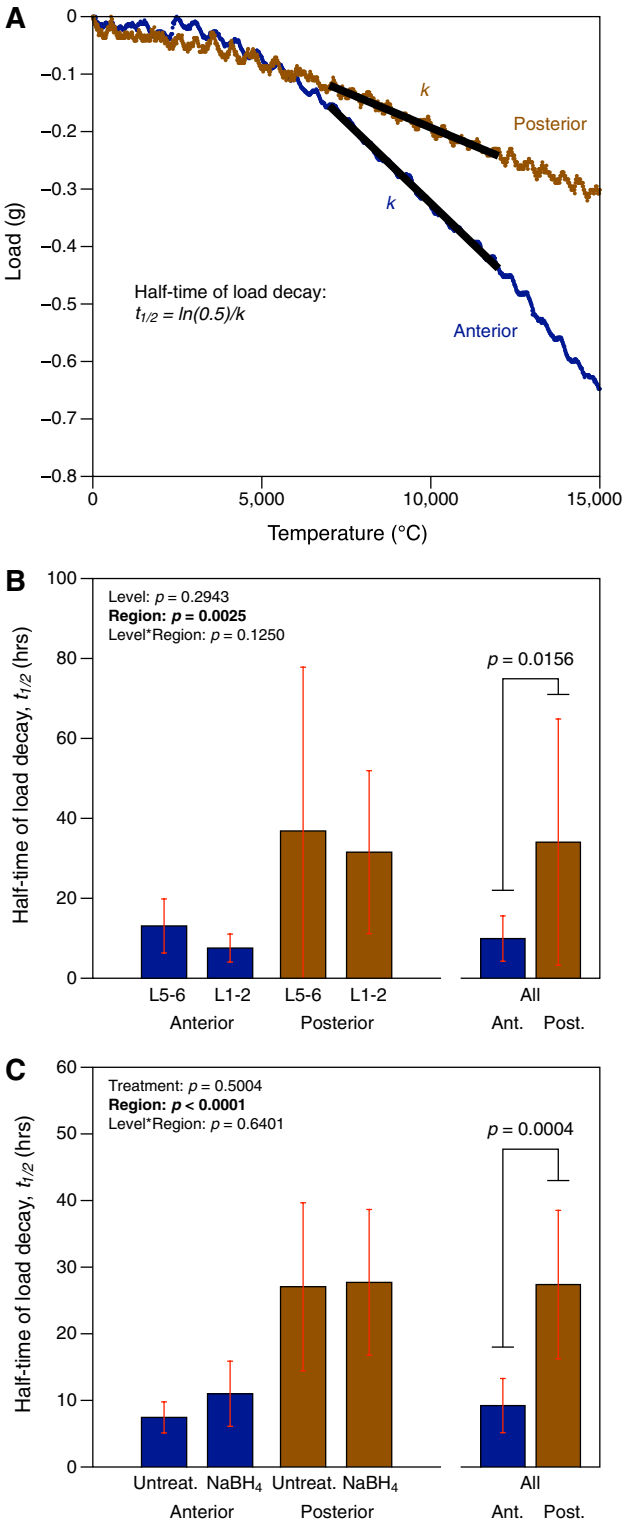

Fig. 3 Collagen intermolecular network integrity, as measured by the isothermal HIT parameter $t_{1/2}$, was significantly greater in the posterior than anterior annulus. **a** Representative HIT responses during the isotherm showing calculation of $t_{1/2}$ for the anterior and posterior portions of a L1–2 disc. **b** Isothermal $t_{1/2}$ data for native samples. **c** Treating samples with $NaBH_4$ to retain thermally labile crosslinks during the 90 °C isotherm did not significantly alter $t_{1/2}$, demonstrating that if present, these crosslinks do not meaningfully contribute to intermolecular network integrity within the annulus

Mechanical testing and light microscopy

Tensile mechanical properties of the anterior and posterior disc wall were assessed using bone-disc-bone samples pulled to rupture, with tension applied parallel to the peripheral annular fibre direction. Ruptured samples were processed into serial cryosections, and failure characteristics were assessed using standard bright-field microscopy.

The L5–6 or L6–7 discs from 13 spines were used for mechanical testing ($n = 13$). Vertebra-disc-vertebra

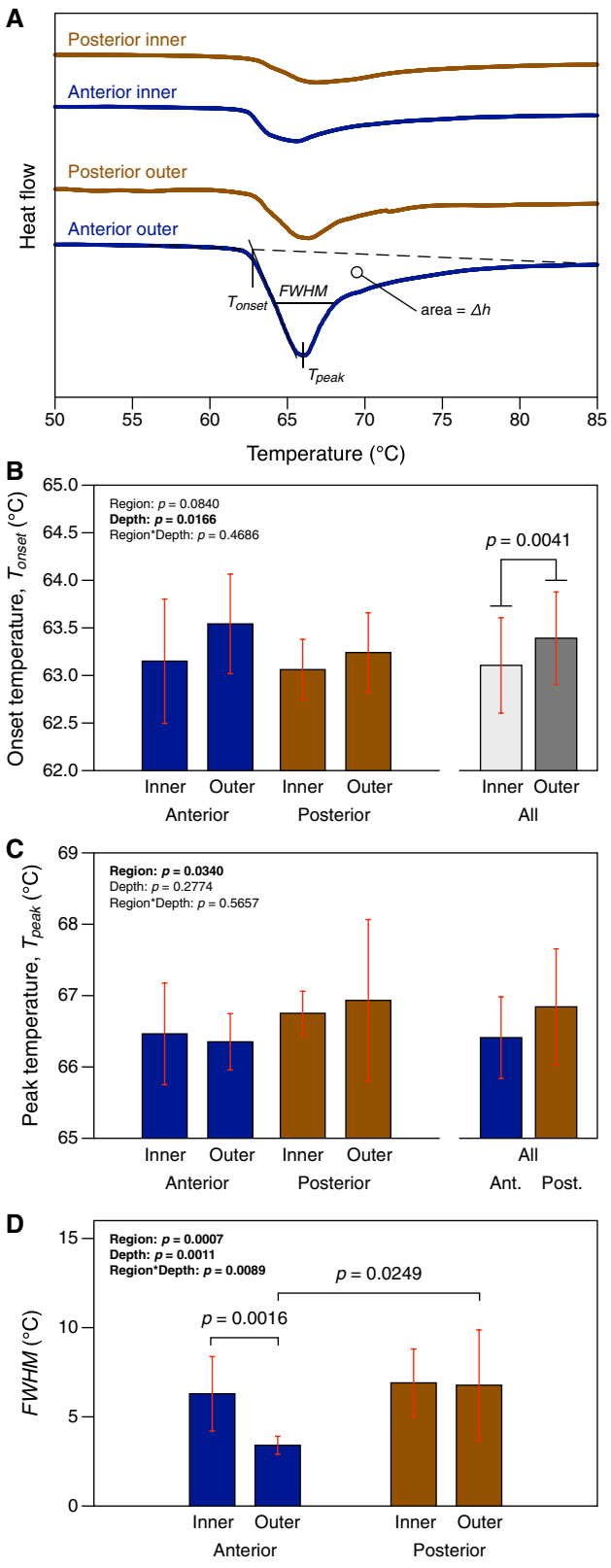

Fig. 4 Unlike HIT, which preferentially measures tension-bearing collagen, fewer regional differences were seen in DSC, which measures the melting energetics of all collagen within a sample regardless of mechanical function. **a** Representative DSC responses for samples from the same L5–6 disc. **b** Minimum collagen thermal stability only varied by radial depth. **c** Thermal stability at maximum heat flow varied by region, but the difference was not significant when samples from both radial depths were pooled. **d** The outer anterior annulus consisted of more homogenously structured collagen, as indicated by FWHM

segments were thawed and residual soft tissues attached to the disc carefully removed by scalpel, including the posterior longitudinal ligament. Each segment was cut coronally using a miniature hacksaw, producing anterior and posterior samples. For the purpose of mounting samples and defining the direction of applied tension, two 5.2-mm-diameter holes were drilled through the superior and inferior vertebral bone with a sagittal offset such that alignment of the holes matched the peripheral fibre orientation of the annulus (Fig. 1). The lateral sides of the annulus were then severed using razor blades, isolating the portion of the annulus located between the mounting holes. On severing the annulus, each blade was temporarily left in position for the purpose of measuring the sample's circumferential width, taken as separation distance between the two blades. Circumferential width was 3.15 ± 0.42 mm for posterior samples and 2.03 ± 0.18 mm for anterior samples.

Mechanical testing was conducted using a servo-hydraulic materials testing system (458 series, MTS, Eden Prairie, MN), with sample hydration maintained via drip-feed of room-temperature PBS. Samples were secured into the system by passing a 5-mm-diameter pin through each mounting hole. Samples were pulled to failure at 0.01 mm/s, while time, displacement, and force data were recorded at 20 Hz. Tests were video-recorded in order to identify cases where vertebral failure at the mounting holes occurred, which happened in two samples. These two samples were excluded from the results.

Following mechanical testing, samples were fixed in 10% neutral-buffered formalin and decalcified in 10% formic acid. Decalcified samples were frozen in liquid nitrogen and cryosectioned using a sliding microtome (model SM2000R, Leica Biosystems, Buffalo Grove, IL) to produce ~ 30-um-thick oblique sagittal sections of both the ruptured disc wall and adjacent untested region (Fig. 1). During cryosectioning, samples were oriented with the section plane parallel to the direction of applied tension during mechanical testing. As a result, lamellar fibres that were in-plane with the applied load were also in-plane in the resulting cryosections. Cryosections were wet mounted and examined unstained using a Nikon Eclipse E600 light microscope with 10-megapixel digital camera.

In order to calculate annular stress during mechanical testing, cryosections adjacent to the tested region of each sample were used to measure the radial thickness of the

annulus (Fig. 1; Supplementary Figure S2). Measurements were made using ImageJ software (version 1.51j8, National Institutes of Health, USA) on panoramic images assembled using PTGui software (version 10.0.15 Pro, New House Internet Services BV, Netherlands). Measurements from multiple cryosections were averaged to provide a single measurement of radial annular thickness for each sample.

Cryosections were also used to confirm skeletal maturity of the spines used. Samples that were found to contain unfused or partially fused vertebral growth plates (three samples) were excluded from the results.

Analysis of mechanical data was done using Microsoft Excel. Stiffness was calculated as the slope of the linear region of the force–displacement response. Stresses were calculated by dividing force data by each sample's circumferential width (measured before testing) and radial thickness of the annulus (measured after testing, using cryosections taken adjacent to the test region). The ultimate tensile strength was the maximum stress recorded. Tension strength of the disc wall was calculated as the maximum force recorded divided by circumferential width.

Statistics

Statistical analyses were conducted using JMP software (version 14, SAS Institute, Cary, NC). Differences between disc levels and annular regions for native HIT samples and DSC samples were assessed using full-factorial, two-way mixed model ANOVA with animal of origin set as the random effect. For the $NaBH_4$-treated and untreated HIT samples, analysis was similar but using the factors annular region and treatment. In cases where the residuals of the model were not normally distributed as determined by Shapiro–Wilk test, the ANOVA was redone using rank transformed data. As appropriate based on ANOVA results and normality of the data, post hoc testing was done by matched-pair *t* test or Wilcoxon signed-rank test. For mechanical data, differences between anterior and posterior samples were tested using matched-pair *t* tests. After assessment of sample failure mode by light microscopy, differences in failure modes between anterior and posterior samples were compared using Fisher's exact test. Differences with $p \leq 0.05$ were considered statistically significant.

Results

Analysis of bone-disc-bone segments using HIT showed that significant differences exist between the collagen nanostructures of the posterior and anterior annulus and that these differences extend over the lumbar spine from L5–6 to L1–2. Denaturation temperature in HIT is a measure of collagen molecular stability, marking the energetic threshold to dissociation of molecular α-chains and subsequent entropically driven generation of tension [20, 22]. At L5–6, samples of anterior annulus had a denaturation temperature of 62.1 ± 1.2 °C while those from the posterior annulus had a denaturation temperature over 4.5 °C higher at 66.8 ± 2.1 °C—a very large difference, in excess of that seen in some tissues throughout development [21]. Similar results were seen at L1–2 (Fig. 2), with statistical analyses confirming no difference between levels, but a significant difference between annular regions ($p < 0.0001$).

Half-time of load decay in HIT, calculated from the isothermal portion of the test, measures intermolecular network integrity of tension-bearing elements within a tissue. With peptide bond hydrolysis gradually occurring along the α-chains of collagen molecules when temperature is held at 90 °C, load decay occurs more gradually in tissues with greater thermally-stable intermolecular crosslinking [23, 24]. For the native samples tested, load decay in the posterior annulus occurred significantly more slowly than in the anterior annulus ($t_{1/2}$ of 32.7 ± 23.7 h for posterior vs. 9.4 ± 4.6 h for anterior; $p = 0.0156$), with no difference between the L5–6 and L1–2 levels (Fig. 3a, b).

With the possibility of divalent aldimine crosslinks existing in the annulus, which are heat labile at temperatures well below 90 °C [13, 25, 26], additional L1–2 samples were tested after treatment using $NaBH_4$, which converts these crosslinks to a heat-stable form [25]. Half-times of load decay for $NaBH_4$-treated L1–2 samples were similar to those of untreated L2–3 samples from the same spine (Fig. 3c). Regardless of treatment, significant differences in load decay were again observed between anterior and posterior regions ($p = 0.0004$), confirming that the total intermolecular network integrity of tension-bearing collagen is greater within the posterior than anterior annulus.

As a compliment to HIT, which only assesses collagen contributing to the tensile load-bearing ability of a sample, DSC assesses the denaturation energetics of all collagen present within a sample regardless of orientation. Representative DSC endotherms from the sample groups assessed are shown in Fig. 4a. Minimum collagen molecular stability, measured by onset temperature, was lower in the inner annulus than outer annulus, with no difference between circumferential regions (Fig. 4b). Peak temperature, which measures molecular stability at maximum heat absorption, only showed variation with circumferential region, though the posterior annulus was not significantly more stable than anterior annulus when results from the inner and outer radial depths were pooled (Fig. 4c). Endotherm full-width at half-maximum measures the level of heterogeneity amongst collagen molecules within a sample, with larger *FWHM* values indicating a greater dispersion of thermal stabilities. The level of molecular heterogeneity in the outer posterior annulus was significantly greater than in the outer

anterior annulus ($p=0.0249$; Fig. 4d). Within the anterior annulus only, molecular heterogeneity was reduced moving from inner annulus to outer annulus ($p=0.0016$). Specific enthalpy of denaturation did not vary significantly with either circumferential region ($p=0.9547$) or radial depth ($p=0.8433$).

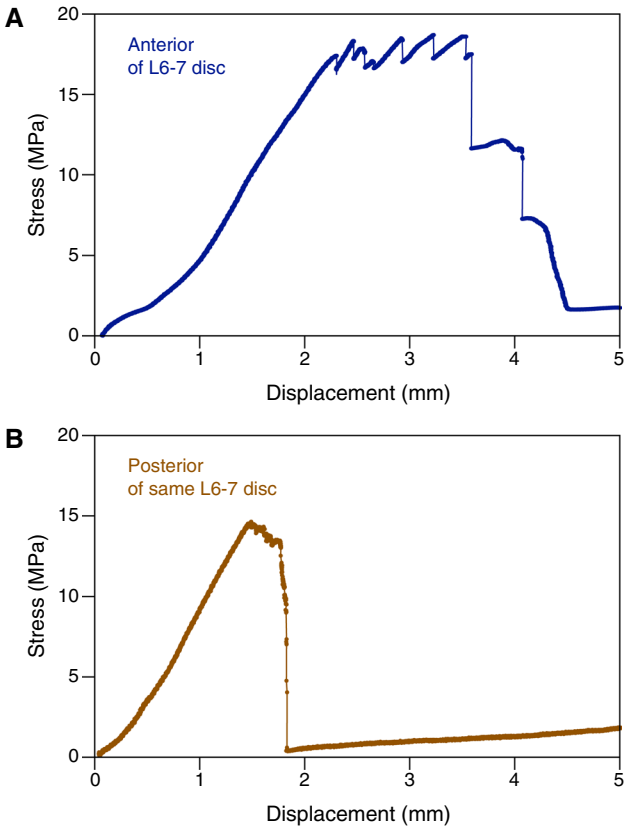

Fig. 5 Representative stress–displacement responses for anterior (**a**) and posterior (**b**) samples from the same L6–7 disc. Bone-disc-bone samples were tested, with tension applied parallel to the peripheral annular fibre orientation. Visible at the top of the plot for the anterior sample are multiple failure events, likely corresponding to sequential failure of fibres from the different in-plane lamellae (i.e. those lamellae with fibres inclined in the direction of applied tension)

Molecular-level differences in collagen structure between anterior and posterior regions of the annulus were accompanied by significant differences in macroscale mechanics. Representative stress–displacement plots of anterior and posterior bone-disc-bone segments pulled to rupture with tension applied parallel to the peripheral annular fibre direction are shown in Fig. 5. Ultimate tensile strength of the anterior disc wall was 19.2 ± 4.0 MPa, significantly greater than that of the posterior disc wall at 12.5 ± 3.3 ($p=0.0312$; Table 1). This already large difference in material properties was amplified to a threefold difference between anterior and posterior regions when annular thickness was used to calculate tension strength of the disc wall per unit of circumferential length: tension strength for the anterior disc wall was 158.0 ± 38.4 N/m versus only 51.4 ± 11.7 for the posterior disc wall ($p=0.0005$). No differences in linear stiffness existed between regions.

Mechanical test samples were cryosectioned and examined unstained and hydrated. Microscopy confirmed that samples had experienced failure within the disc wall, rather than failure by vertebral avulsion. Failure characteristics of the disc wall were similar between anterior and posterior samples. In both regions, the majority of failures were caused by rupture of the tension-carrying in-plane lamella fibres within the disc (Fig. 6). Failure of in-plane fibres at the annulus/cartilage endplate junction or cartilage/vertebral endplate junction was relatively rare, occurring in only 3 of 16 samples (Table 2; Supplementary Figure S3). An interesting feature observed in all anterior and posterior samples was significant damage to those lamellae made up of fibres that were out-of-plane with the applied tensile load, i.e. those that appeared in cross-section in the cryosections. Large segments or isolated portions of cross-sectioned lamellae were often missing (Figs. 7, 8), indicating the occurrence of significant damage to both these lamellae and the adjacent interlamellar junctions. Surprisingly, in many cases this damage extended down to and through the calcified cartilage endplate (arrows in Figs. 7b, 8).

Table 1 Structural and material properties of anterior and posterior regions of the ovine lumbar disc wall

	Anterior disc wall	Posterior disc wall	
Annular thickness (mm)	8.2 ± 0.6	4.2 ± 0.5	***p* < 0.0001**
Stiffness (kN/m)	190.1 ± 48.0	175.3 ± 20.1	$p=0.8690$
Linear slope of stress–displacement curve (GPa/m)	11.9 ± 2.7	13.3 ± 3.7	$p=0.4974$
Tension strength (kN/m)	158.0 ± 38.4	51.4 ± 11.7	***p* = 0.0005**
Ultimate tensile strength (MPa)	19.2 ± 4.0	12.5 ± 3.3	***p* = 0.0312**

Sample size $n=8$ for both groups (of the 13 samples prepared, two were excluded due to vertebral facture at the mounting holes, and three were excluded for lack of skeletal maturity shown by the presence of partially fused growth plates during microscopy). Tension strength is calculated as the maximum force per unit circumferential width

Bold values indicates statistically significant differences of P-values

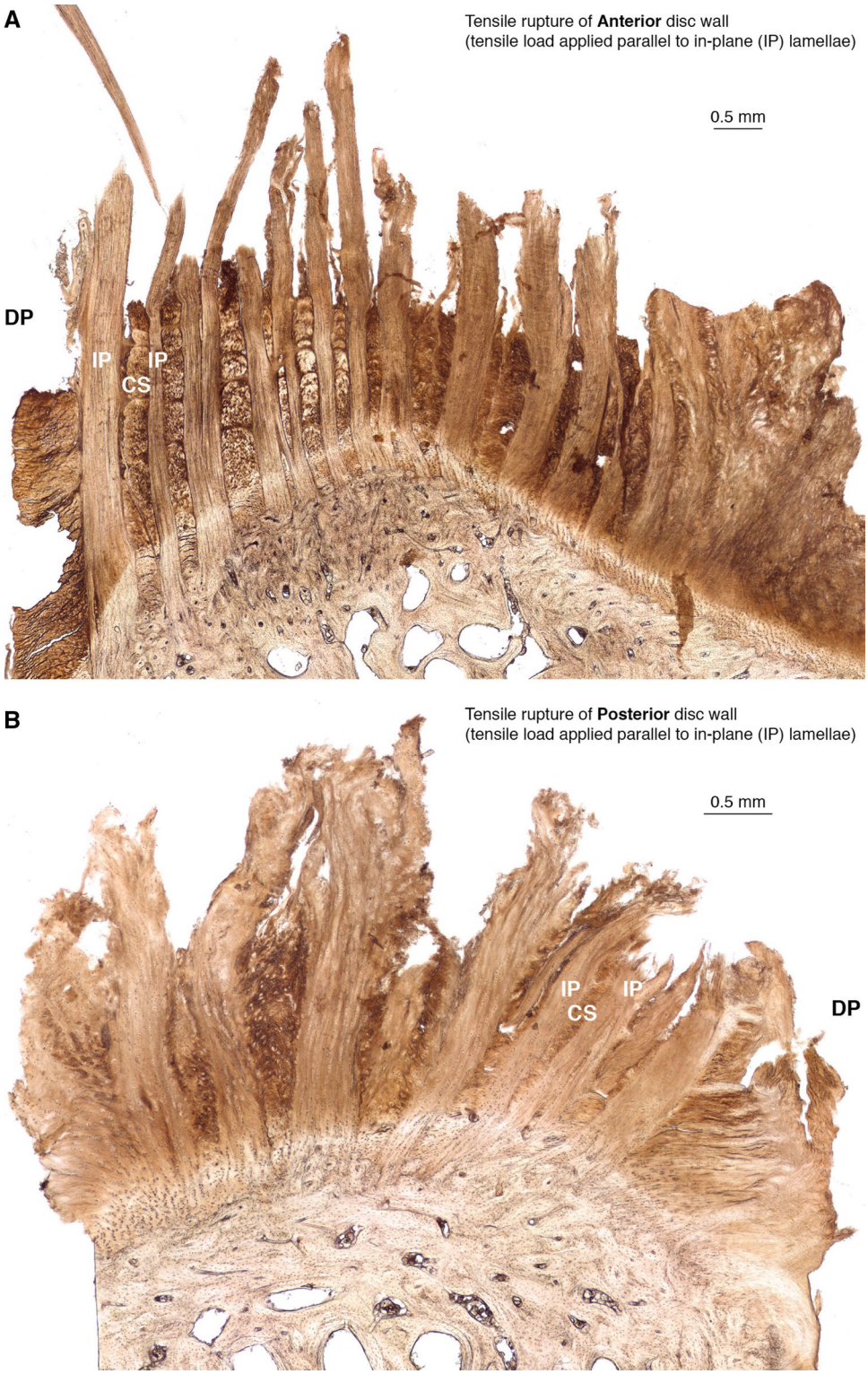

Fig. 6 The majority of samples tested (7/8 anterior and 6/8 posterior) failed by rupture of annular fibres rather than fibre pull-out at the endplate, as shown for these anterior (**a**) and posterior (**b**) samples. Samples were oriented during cryosectioning such that the annular fibres that were aligned with the applied tensile load appear in-plane (IP). Lamellae with fibres that were oriented away from the applied load appear in cross-section (CS). DP indicates the side of the sample at the disc periphery

Discussion

The basic microstructural properties of the lumbar disc annulus are known to vary with circumferential location. Total annular thickness, number of lamellae, and lamella fibre orientation all change moving around the annulus from anterior to posterior [6, 7, 27]. In this study, we have shown that circumferential specialization within annular collagen goes far beyond this, with significant differences in collagen nanostructure present between the disc's anterior and

Table 2 Similar microstructural damage features were observed in anterior and posterior disc wall samples after tension-to-rupture testing

	Anterior disc wall	Posterior disc wall
Rupture of lamellae near mid-disc height	8 of 8	8 of 8
Interlamellar disruption	8 of 8	8 of 8
In-plane lamella pull-out at endplate[a]	1 of 8	2 of 8
Localized damage to cartilage endplate	5 of 8	7 of 8

[a]In-plane lamellae were those containing fibres orientated parallel to the applied tensile load during mechanical testing

posterior. The collagen fibre bundles making up the posterior lamellae are composed of collagen molecules with significantly greater intermolecular network integrity than those forming the anterior annular lamellae. Collagen molecules in the tension-bearing fibre bundles of the posterior annulus also possess significantly greater thermal stability than those in the anterior annulus, indicating important regional differences in the molecular packing structure of collagen fibrils between the two regions. Coincident with differences in collagen nanostructure, significant differences in ultimate tensile strength between the anterior and posterior disc wall also exist. Interestingly, despite the posterior annulus being composed of collagen molecules with greater network integrity and stability, the anterior annulus is significantly stronger. While somewhat counterintuitive, similar results have been reported elsewhere for functionally distinct tissues.

The thermal stability of collagen molecules is dependent on lateral molecular packing density. As isolated monomers, collagen molecules become thermally unstable near 37 °C, undergoing denaturation of the triple helix into random α-chain coils [28]. When packed into a collagen fibril, the conformational entropy of molecules is limited [29], increasing thermal stability by 10 to 15 °C [30]. Intermolecular crosslinking can further increase molecular thermal stability by laterally drawing the adjacent molecules of a fibril together, further decreasing conformational entropy [31]. In the current work, we used two complimentary techniques to measure molecular stability: DSC and HIT. While both techniques measure thermal stability, they do not provide the same information. DSC measures the energetics of the triple helix to random coil denaturation transition for all collagen within a tissue sample [32]. In contrast, HIT measures the initiation of entropically driven contraction upon denaturation for only those molecules that can contribute to axial tension within a sample [33]. The samples prepared for HIT in this study were cut and mounted parallel to one of the annular fibre directions, and hence the tension-bearing annular fibres in this orientation would have preferentially contributed to the signal observed. Matched-pair samples from the anterior and posterior annulus differed in HIT denaturation temperature by an average of 4.6 °C (Fig. 2). In addition to being statistically significant, the magnitude of this difference is large with respect to differences in T_d previously seen between other connective tissues of varying age or function. For example, from foetal development through to adulthood, collagen in the ovine thoracic aorta varies in HIT denaturation temperature by 3.5 °C [21]. In the bovine heart, mitral transvalvular pressure is 144 mmHg, while pulmonary transvalvular pressure is only 12 mmHg. HIT collagen denaturation temperatures in these two tissues differ by 2.7 °C [12]. A similar difference of 2.7 °C is seen between bovine tendons that experience large differences in maximum in vivo stress [13]. That the difference in collagen denaturation temperatures for the anterior and posterior annulus exceeds these is remarkable.

Compared to the dramatic differences seen in thermal stability by HIT, assessments by DSC showed much smaller differences (Fig. 4), with endotherm onset temperature only differing with radial depth and the difference in peak temperature by circumferential region failing to reach significance when samples from both radial depths were pooled. Lack of correspondence between HIT and DSC measurements of thermal stability is not unexpected, as collagen that makes up interlamellar matrix and bridging elements would contribute to signal in DSC but not substantially in HIT. That smaller differences were observed in DSC may indicate structural similarities in these components between regions. While the observed differences in endotherm full width at half maximum are interesting, with indication of greater molecular packing homogeneity present in collagen of the outer anterior annulus compared to outer posterior annulus, it is worth noting that inner and outer anterior samples were separated by a discarded middle section, whereas due to the smaller total annular thickness, inner and outer posterior samples were adjacent to one another.

Total collagen crosslinking within the intervertebral disc annulus has not previously been reported, though some reports on specific crosslinks do exist. Compared to other connective tissues, human annulus has been reported to contain a relatively high concentration of trivalent hydroxylysylpyridinoline (HP) crosslinks [34]. HP crosslinks within the annulus were more thoroughly investigated by Skaggs et al. [35] who reported no regional variation in HP crosslink levels between different regions of human L2–3 discs. With increasing age, Pokharna and Phillips [36] observed a decrease in pyridinoline crosslinks within human lumbar discs along with a simultaneous increase in non-enzymatic pentosidine crosslinks. Brickley-Parsons and Glimcher [37] explored crosslinking within the annulus of human lumbar discs with age, disc level, and annular location, but only assessed reducible

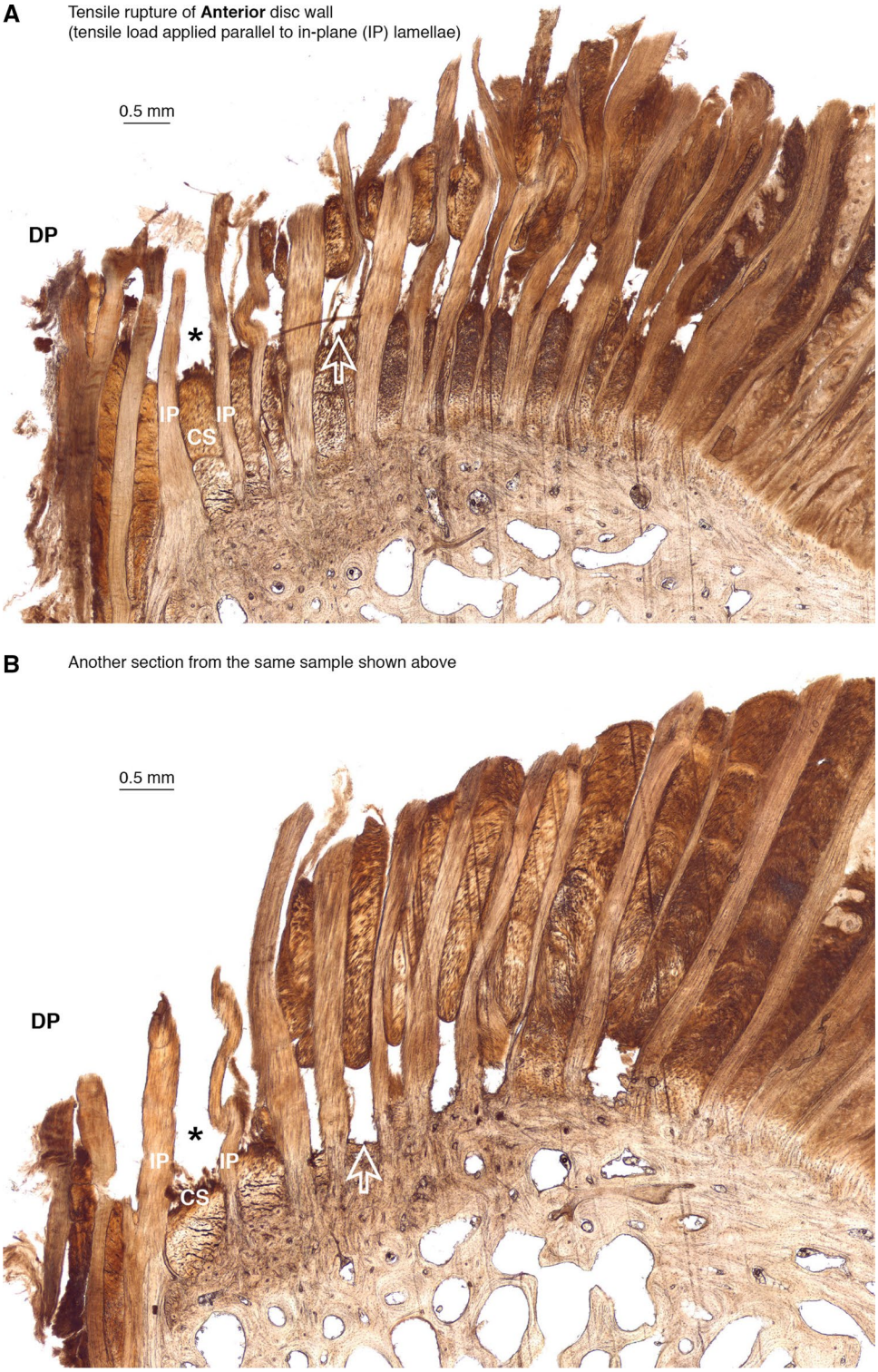

Fig. 7 Damage to interlamellar connections were frequently observed in ruptured anterior (**a**, **b**) and posterior samples (Fig. 8), resulting in loss to portions of cross-sectioned (CS) lamellae that contained fibres out-of-plane with the applied tensile load. Two cryosections from the same L6–7 disc are shown. Loss of large portions of cross-sectioned lamellae in the outer annulus were frequently seen (* in **a**, **b**), and damage to the out-of-plane CS lamellae often extended into the endplate (arrow in **b**). In anterior samples only, over sequential cryosections isolated portions of missing CS lamellae were seen moving from mid-annulus (arrow in **a**) to endplate (arrow in **b**) suggesting that interlamellar damage in the anterior annulus was restricted to a group of one or more annular fibre bundles. DP indicates disc periphery

crosslinks. Two crosslink species were detected: hydroxylysinonorleucine (HLNL) and histidinohydroxymerodesmosine (HHMD). In adult discs, HLNL made up a greater proportion of total reducible crosslinks within the outer posterior annulus compared to the outer anterior annulus, regardless of disc level. While interesting, the data from Brickley-Parsons and Glimcher [37] are marred by long-standing and unresolved debate as to whether HHMD is an artifactual crosslink produced during analysis [38–41]. Such concerns are not unique to HHMD, with the origin of histidinohydroxylysinonorleucine (HHL), long thought to be a native trivalent crosslink, now also under scrutiny

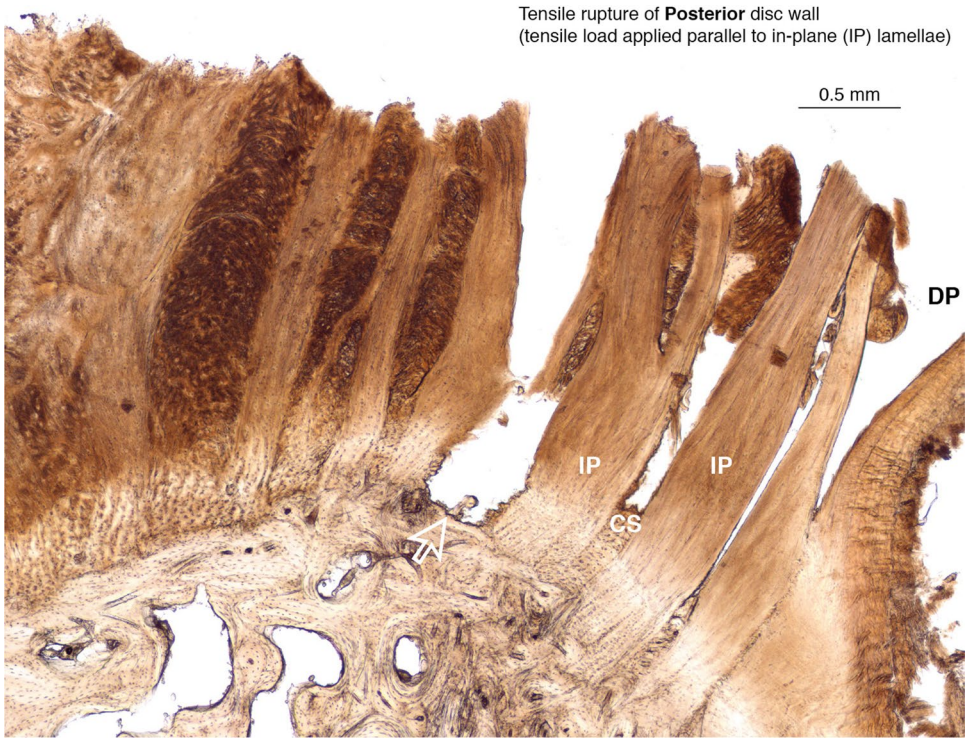

Fig. 8 Damage to interlamellar connections within posterior samples causing loss of the cross-sectioned (CS) lamellae that contained fibres out-of-plane with the applied tensile load often extended into the endplate (arrow), as seen in anterior samples. Unlike anterior samples where interlamellar disruptions that were contained to a group of fibre bundles were frequently observed (Fig. 7), interlamellar damage in the posterior annulus usually resulted in complete loss of the CS lamellae. DP indicates disc periphery. The cryosection shown is from a ruptured L6–7 sample

[42, 43]. Clearly, a complete description of native collagen crosslinking within the annulus does not yet exist.

Assessing collagen crosslinking is of interest due to the crucial mechanical role that crosslinking plays in creating intermolecular network integrity within the collagen hierarchy [44–46]. Rather than inferring intermolecular network integrity from quantitatively-derived crosslink concentrations, which may not show correspondence in mature tissues [47], measuring isothermal load decay using HIT assesses intermolecular network integrity directly [23, 24]. Moreover, the nature of HIT provides functional assessment: only those tissue components that contribute to axial tension within a sample are measured. At the start of the HIT isotherm, the level of tension produced by a sample is dependent on the number of collagen molecules that are functionally interconnected between the system's grips, with tension contributed by these molecules' entropic desire to randomly coil in a thermal environment exceeding the denaturation temperature [33]. During the isotherm, as peptide bond hydrolysis occurs along collagen α-chains load follows a Maxwell decay, with the rate of decay depending on the level of intermolecular network integrity present [48]. Our isothermal HIT assessments in the current study provide three significant results. First, intermolecular network integrity within the collagen fibre bundles of the posterior annulus is significantly greater than that in the anterior annulus (Fig. 3b). Second, this regional difference is present throughout the lumbar spine. Third, the contribution to intermolecular network integrity from thermally labile, reducible crosslinks like HLNL is negligible (Fig. 3c).

Given that our results show greater intermolecular network integrity within the posterior compared to anterior annulus, it may seem odd that the posterior annulus was found to be significantly weaker (Table 1, Fig. 5). It is well accepted that during tissue development increases in crosslinking lead to increases in tissue strength [49, 50]. Similarly, inhibition of crosslinking reduces strength [44]. Beyond development, however, relationships between crosslinking and mechanics are less clear. For instance, Hansen et al. [47] studied both crosslinking and mechanics of anterior and posterior fascicles from the patellar tendons of healthy young men. Despite anterior fascicles being significantly stiffer and stronger, no correspondence was found between crosslink concentrations and mechanical properties. Couppé et al. [51] studied the patellar tendons of young and older men and found no differences in mechanical properties despite the tendons of older men having significantly greater levels of both enzymatic and non-enzymatic crosslinking. Beyond these studies showing no relationship between mechanics and crosslinking, inverse relationships have been documented for other mature tissues. Forelimb tendons from quadrupeds have been particularly useful for exploring collagen structure–function relationships, with anatomically proximate but physiologically distinct tendons present within several frequently used models (horses, cows, and sheep). In both the equine and bovine forelimbs, for example, the superficial digital flexor tendon sustains

significantly higher maximum in vivo stress compared to the digital extensor tendons: 75 versus 15–36 MPa for the equine tendons, and 69 versus 8–11 MPa for the bovine tendons [52]. Despite the equine superficial digital flexor tendon sustaining significantly greater in vivo stresses and containing significantly denser HP crosslinking, the common digital extensor tendon is stronger [53]. Similar results have been reported for the bovine forelimb tendons: despite flexor tendons possessing significantly greater intermolecular network integrity, extensor tendons are stronger [13, 18]. Tendons from the ovine forelimb have shown results consistent with those from the equine and bovine models [54]. In these cases, the higher strength of the less crosslinked tendons may be in part due to an increased ability amongst their constituent collagen fibrils to more evenly share load by undergoing significant plastic deformation [15, 16, 55]. In contrast, the more heavily crosslinked tendons show significantly better fatigue resistance under cyclic loading, accumulating damage at a reduced rate [13, 18]. Considering these previous findings, the results of the current study suggest that the collagen nanostructure of the posterior annulus may have developed for increased fatigue resistance at the expense of tensile strength.

In relation to previous disc research, our mechanical findings indicate that tensile strength of the disc wall may be more than double previously reported values. As well as being of high significance to the many modelling studies of disc failure that are conducted, such information is important to the design of annular repair strategies and devices. To retain structural integrations, we prepared and tested bone-disc-bone samples in the current study. These were loaded along one of the principal annular fibre directions, providing a measurement of the disc wall's tensile properties with minimal intralamellar shear (Fig. 1). For testing conducted to failure, we are not aware of prior reports using this preparation. Green et al. [56] and Zak and Pezowicz [57] both prepared bone-disc-bone samples for tension-to-rupture testing, but loaded samples vertically. Green et al. [56] reported ultimate strengths of 1.7 and 3.8 MPa for anterior and posterior samples, respectively, while Zak and Pezowicz [57] reported 7.5 and 4.5 MPa for the same two regions. Two studies have attempted to determine annular strengths by applying tension parallel to one of the annulus' primary fibre directions, but have done so using isolated samples of annulus. With annular fibres under considerable residual stress when integrated into the disc wall [58, 59], severing annular connections to the vertebrae likely results in structurally compromised test samples. Perhaps unsurprisingly, those studies have also reported values of annular strength significantly smaller than those reported here, with Shan et al. [60] reporting strength values of 3.5 and 3.1 MPa for the anterior and posterolateral annulus, respectively, and Skaggs et al. [35] reporting 10.3 and 5.6 MPa for the same two values. In comparison, we measured ultimate tensile strengths of 19.2 ± 4.0 and 12.5 ± 3.3 MPa for the anterior and posterior disc wall (Table 1). It is worth noting that the cross-sectional areas used for these measurements include those lamellae oriented away from the axis of tensile loading. Consequently, the true tensile strength of annular fibres would be substantially higher than the values that we report (perhaps nearly double), far in excess of those previously reported.

On microscopic examination of the ruptured disc wall samples, one of the most common features observed in the current study was disruption to those lamellae with fibres oriented away from the direction of applied tension. In the tissue sections examined, portions of these lamellae were frequently missing (Figs. 7, 8), with fibre bundles and/or interlamellar connections having been damaged to the point where the tissue lacked connectivity to adjacent structures and was lost when the freshly cut sections were placed in solution. Clearly, under loading situations that selectively strain annular fibres in only one direction, as in axial rotations, the resulting interlamellar shear stresses can significantly disrupt interlamellar connections. Such loading situations are therefore likely to be strong contributors to the development of circumferential tears. While circumferential tears on their own may not be of significant interest from a pain or disability standpoint, they are frequently connected to by radial tears [61–63] and thus may influence characteristics associated with nuclear migration like protrusion location or extent [64], making them of clinical interest. It is interesting to note that although the collagen fibre bundles of the anterior annulus possess significantly greater ultimate tensile strength than those of the posterior annulus, similar regional differences in interlamellar shear strength do not appear to exist [65], consistent with observations showing similar instances of circumferential tears in the posterior and anterior annulus [10, 11, 66].

There are a few limitations that should be mentioned regarding the work presented. First, the work was conducted using an ovine model. The study used a total of 38 motion segments from 23 spines. Obtaining that quantity of healthy human tissue was simply not feasible. That said, the ovine lumbar spine has been well compared to the human lumbar spine. In addition to biomechanics [67–69], disc shape [67], and disc biochemical composition comparing favourably [19, 68, 69], perhaps most relevant to the current work is the level of microstructural correspondence that has been shown to exist. Annular fibre angles have been found to be similar in both human and ovine lumbar discs [19], and the presence of microstructurally comparable cross-bridges has been documented in the lumbar discs from both species [70, 71]. Structural integration from annulus through to vertebrae is also similar, with annular fibres anchoring into calcified cartilage

endplate in both species, and further into the vertebral endplate within the outer annulus [72–74]. Despite these similarities, it should be recognized that the human annulus of even young adults would be expected to contain levels of advanced glycation endproduct (AGE) crosslinks far beyond those normally found in skeletally mature sheep. In tendon, while AGEs have been found to modestly increase the molecular stability of collagen [55], they do not appear to alter suboverload mechanics [51, 75], and, depending on the level of enzymatic crosslinking present, may not alter ultimate tensile strength despite significantly affecting ultrastructural failure characteristics [55]. How the presence of increasing levels of AGEs affects annular mechanics has not yet been well studied and was beyond the scope of the current research. Finally, it should be recognized that the method of mechanical sample preparation employed would have resulted in lower tensile stresses at the endplate compared to those present at mid-disc height where the razor cuts used to define each sample's circumferential width were positioned. Thus, while very few of our samples involved endplate failures, this cannot be taken as proof that the tensile strengths of annulus/endplate integrations exceed those of the annular fibres themselves.

Conclusion

Collagen of the lumbar intervertebral disc annulus shows circumferential regional specialization in structure at the fundamental, nanoscale level. Compared to the anterior annulus, the posterior annulus, which experiences larger tensile strains during daily living, is composed of collagen molecules with greater thermal stability and intermolecular network integrity. Despite possessing a seemingly more robust collagen nanostructure, the posterior annulus is significantly weaker than the anterior annulus. As seen for other tissues with similar differences in collagen nanostructure, the posterior annulus may have evolved for improved fatigue resistance at the expense of strength.

Acknowledgements This work was supported by a grant to SPV from the Nova Scotia Health Research Foundation. TWH acknowledges stipend funding support from the Natural Sciences and Engineering Research Council of Canada (NSERC). We acknowledge the support of the Canada Foundation for Innovation, the Atlantic Innovation Fund, and other partners which fund the Facilities for Materials Characterization, managed by the Clean Technologies Research Institute, Dalhousie University.

Compliance with ethical standards

Conflict of interest All authors declare that they have no conflict of interest.

References

1. Alexander LA, Hancock E, Agouris I et al (2007) The response of the nucleus pulposus of the lumbar intervertebral discs to functionally loaded positions. Spine 32:1508–1512. https://doi.org/10.1097/BRS.0b013e318067dccb
2. Fennell AJ, Jones AP, Hukins DW (1996) Migration of the nucleus pulposus within the intervertebral disc during flexion and extension of the spine. Spine 21:2753–2757. https://doi.org/10.1097/00007632-199612010-00009
3. Wilke HJ, Neef P, Caimi M et al (1999) New in vivo measurements of pressures in the intervertebral disc in daily life. Spine 24:755–762. https://doi.org/10.1097/00007632-199904150-00005
4. Kelsey JL, Githens PB, White AA et al (1984) An epidemiologic study of lifting and twisting on the job and risk for acute prolapsed lumbar intervertebral disc. J Orthop Res 2:61–66. https://doi.org/10.1002/jor.1100020110
5. Veres SP, Robertson PA, Broom ND (2010) The influence of torsion on disc herniation when combined with flexion. Eur Spine J 19:1468–1478. https://doi.org/10.1007/s00586-010-1383-0
6. Tsuji H, Hirano N, Ohshima H et al (1993) Structural variation of the anterior and posterior anulus fibrosus in the development of human lumbar intervertebral disc. A risk factor for intervertebral disc rupture. Spine 18:204–210
7. Marchand F, Ahmed AM (1990) Investigation of the laminate structure of lumbar disc anulus fibrosus. Spine 15:402–410. https://doi.org/10.1097/00007632-199005000-00011
8. Schmidt H, Kettler A, Heuer F et al (2007) Intradiscal pressure, shear strain, and fiber strain in the intervertebral disc under combined loading. Spine 32:748–755. https://doi.org/10.1097/01.brs.0000259059.90430.c2
9. Moore RJ, Vernon-Roberts B, Fraser RD et al (1996) The origin and fate of herniated lumbar intervertebral disc tissue. Spine 21:2149–2155
10. Osti OL, Vernon-Roberts B, Moore R, Fraser RD (1992) Annular tears and disc degeneration in the lumbar spine. A post-mortem study of 135 discs. J Bone Joint Surg Br 74:678–682
11. Vernon-Roberts B, Moore RJ, Fraser RD (2007) The natural history of age-related disc degeneration: the pathology and sequelae of tears. Spine 32:2797–2804. https://doi.org/10.1097/BRS.0b013e31815b64d2
12. Aldous IG, Veres SP, Jahangir A, Lee JM (2009) Differences in collagen cross-linking between the four valves of the bovine heart: a possible role in adaptation to mechanical fatigue. Am J Physiol Heart Circ Physiol 296:H1898–H1906. https://doi.org/10.1152/ajpheart.01173.2008
13. Herod TW, Chambers NC, Veres SP (2016) Collagen fibrils in functionally distinct tendons have differing structural responses to tendon rupture and fatigue loading. Acta Biomater 42:296–307. https://doi.org/10.1016/j.actbio.2016.06.017
14. Birch HL, Thorpe CT, Rumian AP (2013) Specialisation of extracellular matrix for function in tendons and ligaments. Muscles Ligaments Tendons J 3:12–22. https://doi.org/10.11138/mltj/2013.3.1.012
15. Chambers NC, Herod TW, Veres SP (2018) Ultrastructure of tendon rupture depends on strain rate and tendon type. J Orthop Res 36:2842–2850. https://doi.org/10.1002/jor.24067
16. Quigley AS, Bancelin S, Deska-Gauthier D et al (2018) In tendons, differing physiological requirements lead to functionally distinct nanostructures. Sci Rep 8:4409. https://doi.org/10.1038/s41598-018-22741-8
17. Svensson RB, Mulder H, Kovanen V, Magnusson SP (2013) Fracture mechanics of collagen fibrils: influence of natural cross-links. Biophys J 104:2476–2484. https://doi.org/10.1016/j.bpj.2013.04.033

18. Shepherd JH, Legerlotz K, Demirci T et al (2014) Functionally distinct tendon fascicles exhibit different creep and stress relaxation behaviour. Proc Inst Mech Eng H 228:49–59. https://doi.org/10.1177/0954411913509977
19. Reid JE, Meakin JR, Robins SP et al (2002) Sheep lumbar intervertebral discs as models for human discs. Clin Biomech (Bristol Avon) 17:312–314
20. Lee JM, Pereira CA, Abdulla D et al (1995) A multi-sample denaturation temperature tester for collagenous biomaterials. Med Eng Phys 17:115–121
21. Wells SM, Adamson SL, Langille BL, Lee JM (1998) Thermomechanical analysis of collagen crosslinking in the developing ovine thoracic aorta. Biorheology 35:399–414
22. Weiderhorn NM, Reardon GV (1952) Studies concerned with the structure of collagen. II. Stress-strain behavior of thermally contracted collagen. J Polym Sci 9:315–325
23. Naimark WA, Waldman SD, Anderson RJ et al (1998) Thermomechanical analysis of collagen crosslinking in the developing lamb pericardium. Biorheology 35:1–16. https://doi.org/10.1016/S0006-355X(98)00016-X
24. Le Lous M, Cohen-Solal L, Allain JC et al (1985) Age related evolution of stable collagen reticulation in human skin. Connect Tissue Res 13:145–155
25. Bailey AJ, Lister D (1968) Thermally labile cross-links in native collagen. Nature 220:280–281
26. Avery NC, Bailey AJ (2008) Restraining cross-links responsible for the mechanical properties of collagen fibers: natural and artificial. In: Fratzl P (ed) Collagen structure and mechanics. Springer, Boston, pp 81–110
27. Holzapfel GA, Schulze-Bauer CAJ, Feigl G, Regitnig P (2005) Single lamellar mechanics of the human lumbar anulus fibrosus. Biomech Model Mechanobiol 3:125–140. https://doi.org/10.1007/s10237-004-0053-8
28. Leikina E, Mertts MV, Kuznetsova N, Leikin S (2002) Type I collagen is thermally unstable at body temperature. Proc Natl Acad Sci USA 99:1314–1318. https://doi.org/10.1073/pnas.032307099
29. Miles CA, Ghelashvili M (1999) Polymer-in-a-box mechanism for the thermal stabilization of collagen molecules in fibers. Biophys J 76:3243–3252. https://doi.org/10.1016/S0006-3495(99)77476-X
30. Wallace DG, Condell RA, Donovan JW et al (1986) Multiple denaturational transitions in fibrillar collagen. Biopolymers 25:1875–1895. https://doi.org/10.1002/bip.360251006
31. Miles CA, Avery NC, Rodin VV, Bailey AJ (2005) The increase in denaturation temperature following cross-linking of collagen is caused by dehydration of the fibres. J Mol Biol 346:551–556. https://doi.org/10.1016/j.jmb.2004.12.001
32. Miles CA, Burjanadze TV, Bailey AJ (1995) The kinetics of the thermal denaturation of collagen in unrestrained rat tail tendon determined by differential scanning calorimetry. J Mol Biol 245:437–446. https://doi.org/10.1006/jmbi.1994.0035
33. Allain JC, Le Lous M, Cohen-Solal L et al (1980) Isometric tensions developed during the hydrothermal swelling of rat skin. Connect Tissue Res 7:127–133. https://doi.org/10.3109/03008208009152104
34. Eyre DR, Koob TJ, Van Ness KP (1984) Quantitation of hydroxypyridinium crosslinks in collagen by high-performance liquid chromatography. Anal Biochem 137:380–388
35. Skaggs DL, Weidenbaum M, Iatridis JC et al (1994) Regional variation in tensile properties and biochemical composition of the human lumbar anulus fibrosus. Spine 19:1310–1319
36. Pokharna HK, Phillips FM (1998) Collagen crosslinks in human lumbar intervertebral disc aging. Spine 23:1645–1648. https://doi.org/10.1097/00007632-199808010-00005
37. Brickley-Parsons D, Glimcher MJ (1984) Is the chemistry of collagen in intervertebral discs an expression of Wolff's Law? A study of the human lumbar spine. Spine 9:148–163. https://doi.org/10.1097/00007632-198403000-00005
38. Robins SP, Bailey AJ (1977) The chemistry of the collagen cross-links. Characterization of the products of reduction of skin, tendon and bone with sodium cyanoborohydride. Biochem J 163:339–346. https://doi.org/10.1080/00223980.2014.996512
39. Robins SP, Bailey AJ (1973) The chemistry of the collagen cross-links. The characterization of fraction C, a possible artifact produced during the reduction of collagen fibres with borohydride. Biochem J 135:657–665
40. Bernstein PH, Mechanic GL (1980) A natural histidine-based imminium cross-link in collagen and its location. J Biol Chem 255:10414–10422
41. Avery NC, Bailey AJ (2005) Enzymic and non-enzymic cross-linking mechanisms in relation to turnover of collagen: relevance to aging and exercise. Scand J Med Sci Sports 15:231–240. https://doi.org/10.1111/j.1600-0838.2005.00464.x
42. Yamauchi M, Taga Y, Terajima M (2019) Analyses of lysine aldehyde cross-linking in collagen reveal that the mature cross-link histidinohydroxylysinonorleucine is an artifact. J Biol Chem 294:14163–14163. https://doi.org/10.1074/jbc.RA118.007202
43. Eyre DR, Weis M, Rai J (2019) Analyses of lysine aldehyde cross-linking in collagen reveal that the mature cross-link histidinohydroxylysinonorleucine is an artifact. J Biol Chem. https://doi.org/10.1074/jbc.RA118.007202
44. Haut RC (1985) The effect of a lathyritic diet on the sensitivity of tendon to strain rate. J Biomech Eng 107:166–174
45. Marturano JE, Arena JD, Schiller ZA et al (2013) Characterization of mechanical and biochemical properties of developing embryonic tendon. Proc Natl Acad Sci USA 110:6370–6375. https://doi.org/10.1073/pnas.1300135110
46. Paschalis EP, Tatakis DN, Robins S et al (2011) Lathyrism-induced alterations in collagen cross-links influence the mechanical properties of bone material without affecting the mineral. Bone 49:1232–1241. https://doi.org/10.1016/j.bone.2011.08.027
47. Hansen P, Haraldsson BT, Aagaard P et al (2010) Lower strength of the human posterior patellar tendon seems unrelated to mature collagen cross-linking and fibril morphology. J Appl Physiol 108:47–52. https://doi.org/10.1152/japplphysiol.00944.2009
48. Le Lous M, Allain JC, Cohen-Solal L, Maroteaux P (1982) The rate of collagen maturation in rat and human skin. Connect Tissue Res 9:253–262
49. Bailey AJ (1968) Intermediate labile intermolecular crosslinks in collagen fibres. Biochim Biophys Acta 160:447–453
50. Torp S, Arridge RGC, Armeniades CD, Baer E (1975) Structure–property relationships in tendon as a function of age. Struct Fibrous Biopolym 26:197–221
51. Couppé C, Hansen P, Kongsgaard M et al (2009) Mechanical properties and collagen cross-linking of the patellar tendon in old and young men. J Appl Physiol 107:880–886. https://doi.org/10.1152/japplphysiol.00291.2009
52. Ker RF, Alexander R, Bennett MB (1988) Why are mammalian tendons so thick? J Zool 216:309–324
53. Thorpe CT, Udeze CP, Birch HL et al (2012) Specialization of tendon mechanical properties results from interfascicular differences. J R Soc Interface 9:3108–3117. https://doi.org/10.1098/rsif.2012.0362
54. Choi RK, Smith MM, Smith S et al (2019) Functionally distinct tendons have different biomechanical, biochemical and histological responses to in vitro unloading. J Biomech. https://doi.org/10.1016/j.jbiomech.2019.109321
55. Lee JM, Veres SP (2019) Advanced glycation end-product cross-linking inhibits biomechanical plasticity and characteristic failure morphology of native tendon. J Appl Physiol 126:832–841. https://doi.org/10.1152/japplphysiol.00430.2018

56. Green TP, Adams MA, Dolan P (1993) Tensile properties of the annulus fibrosus II. Ultimate tensile strength and fatigue life. Eur Spine J 2:209–214
57. Zak M, Pezowicz C (2013) Spinal sections and regional variations in the mechanical properties of the annulus fibrosus subjected to tensile loading. Acta Bioeng Biomech 15:51–59. https://doi.org/10.5277/abb130107
58. Michalek AJ, Gardner-Morse MG, Iatridis JC (2012) Large residual strains are present in the intervertebral disc annulus fibrosus in the unloaded state. J Biomech 45:1227–1231. https://doi.org/10.1016/j.jbiomech.2012.01.042
59. Duclos SE, Michalek AJ (2017) Residual strains in the intervertebral disc annulus fibrosus suggest complex tissue remodeling in response to in-vivo loading. J Mech Behav Biomed Mater 68:232–238. https://doi.org/10.1016/j.jmbbm.2017.02.010
60. Shan Z, Li S, Liu J et al (2015) Correlation between biomechanical properties of the annulus fibrosus and magnetic resonance imaging (MRI) findings. Eur Spine J 24:1909–1916. https://doi.org/10.1007/s00586-015-4061-4
61. Ninomiya M, Muro T (1992) Pathoanatomy of lumbar disc herniation as demonstrated by computed tomography/discography. Spine 17:1316–1322. https://doi.org/10.1097/00007632-199211000-00010
62. Aprill C, Bogduk N (1992) High-intensity zone: a diagnostic sign of painful lumbar disc on magnetic resonance imaging. Br J Radiol 65:361–369. https://doi.org/10.1259/0007-1285-65-773-361
63. Ohnmeiss DD, Vanharanta H, Ekholm J (1999) Relation between pain location and disc pathology: a study of pain drawings and CT/discography. Clin J Pain 15:210–217
64. Rajasekaran S, Bajaj N, Tubaki V et al (2013) ISSLS Prize winner: The anatomy of failure in lumbar disc herniation: an in vivo, multimodal, prospective study of 181 subjects. Spine 38:1491–1500. https://doi.org/10.1097/BRS.0b013e31829a6fa6
65. Gregory DE, Bae WC, Sah RL, Masuda K (2012) Anular delamination strength of human lumbar intervertebral disc. Eur Spine J 21:1716–1723. https://doi.org/10.1007/s00586-012-2308-x
66. Kakitsubata Y, Theodorou DJ, Theodorou S et al (2003) Magnetic resonance discography in cadavers: tears of the annulus fibrosus. Clin Orthop Relat Res 407:228–240. https://doi.org/10.1097/01.blo.0000030506.43495.d4
67. Easley NE, Wang M, McGrady LM, Toth JM (2008) Biomechanical and radiographic evaluation of an ovine model for the human lumbar spine. Proc Inst Mech Eng H 222:915–922. https://doi.org/10.1243/09544119JEIM345
68. Beckstein JC, Sen S, Schaer TP et al (2008) Comparison of animal discs used in disc research to human lumbar disc: axial compression mechanics and glycosaminoglycan content. Spine 33:E166–E173. https://doi.org/10.1097/BRS.0b013e318166e001
69. Showalter BL, Beckstein JC, Martin JT et al (2012) Comparison of animal discs used in disc research to human lumbar disc: torsion mechanics and collagen content. Spine 37:E900–E907. https://doi.org/10.1097/BRS.0b013e31824d911c
70. Schollum ML, Schollum ML, Robertson PA et al (2009) A microstructural investigation of intervertebral disc lamellar connectivity: detailed analysis of the translamellar bridges. J Anat. https://doi.org/10.1111/j.1469-7580.2009.01076.x
71. Smith LJ, Elliott DM (2011) Formation of lamellar cross bridges in the annulus fibrosus of the intervertebral disc is a consequence of vascular regression. Matrix Biol 30:267–274. https://doi.org/10.1016/j.matbio.2011.03.009
72. Brown S, Rodrigues S, Sharp C et al (2017) Staying connected: structural integration at the intervertebral disc-vertebra interface of human lumbar spines. Eur Spine J 26:248–258. https://doi.org/10.1007/s00586-016-4560-y
73. Rodrigues SA, Thambyah A, Broom ND (2017) How maturity influences annulus-endplate integration in the ovine intervertebral disc: a micro- and ultra-structural study. J Anat 230:152–164. https://doi.org/10.1111/joa.12536
74. Rodrigues SA, Thambyah A, Broom ND (2015) A multiscale structural investigation of the annulus-endplate anchorage system and its mechanisms of failure. Spine J 15:405–416. https://doi.org/10.1016/j.spinee.2014.12.144
75. Gautieri A, Passini FS, Silván U et al (2017) Advanced glycation end-products: Mechanics of aged collagen from molecule to tissue. Matrix Biol 59:95–108. https://doi.org/10.1016/j.matbio.2016.09.001

Affiliations

Tyler W. Herod[1] · Samuel P. Veres[1,2]

✉ Samuel P. Veres
sam.veres@smu.ca

[1] School of Biomedical Engineering, Dalhousie University, Halifax, Canada

[2] Division of Engineering, Saint Mary's University, Halifax, Canada